17

Wideband Antennas for Modern Radar Systems

Yu-Jiun Ren and Chieh-Ping Lai
Advanced A&M Technologies, Inc.
U.S.A.

1. Introduction

Wideband antennas have received much attention in wireless communications and broadcasting systems. With a wide bandwidth, the signals can be transmitted by ultra-short impulses or by using multi-band groups. More information and applications can be carried through the radio frequency channels with a high data rate and accuracy. Also, there are numerous military and commercial sensing systems that require wide bandwidth to increase the range accuracy, imaging resolution, jamming/anti-jamming, and hardware flexibility. For various modern radars, such as air defense, air traffic control, astronomy, Doppler navigation, terrain avoidance, and weather mapping, the design of wideband antennas would have different considerations and specifications in order to meet the requirements of specified signals and waveforms.

The key issues of emerging radar antennas are low-profile, low cost, conformal, and compact design. Currently many researchers focus on omni-directional wideband antennas because their widely-covered beamwidth enables them to detect and communicate with targets anywhere. However, this may cause the radar to confuse where the target is located. Therefore, in certain aspects, directional antennas present more interest. The effective isotropic radiated power of a directional antenna is directed to reduce power consumption at the transmitter. This is also beneficial for the receiver's link budget. According to the radar range equation, the antennas can significantly determine the radar performance owing to its power handling, aperture dimension, beamwidth resolution, and potentials of beamforming and scanning. It may spend large amount of the budget for the antenna system cost depending on required functions.

In this chapter, we investigate state of the art wideband radar antennas and focus on applications for airborne radars, ground penetrating radars, noise radars, and UWB radars. The design concepts and considerations of these antennas will be addressed. Following the performance overview of these antennas, we introduce state of the art wideband antennas recently developed for new radar applications. Design details, examples, and profiles of the wideband antennas will be reviewd and discussed.

2. Antenna design and performance requirements

In this section, we introduce important parameters to describe the antenna performance. Instead of theoretically deriving them, we just simply pose these parameters and connect

them with performance. Here, only basic antenna knowledge for understanding the characteristics of antenna and array antenna will be presented.

2.1 Antenna basics

Before knowing the antenna basic parameters, we should know in what range the antenna works in its normal function. The radiation filed close to the antenna includes both radiation energy and reactive energy. For most radar applications, the target is far from the antenna that satisfies the far-field region condition. In this region, only the radiating energy is present and the power variation is related to direction, independent of distance, which is at a radius R given by

$$R = 2L^2/\lambda \tag{1}$$

where L is the diameter of the antenna and λ is the free space wavelength of the operation frequency. Within that radius is the near-field region (Fresnel region) in which the radiation field changes rapidly. In the far-field region (Fraunhofer region), the wavefronts are actually spherical, but a small section of the wavefronts can be approximately considered as a plane wave. This way, only the power radiated to a particular direction is concerned, instead of the shape of the antenna. The above condition is determined based on the error due to distance phase ($< \pi/8$) from the observing point to the antenna. If requiring more accurate phase, the far-field radius has to be increased (Balanis, 1982).

The radiation pattern is a plot of the power radiated from the antenna per unit solid angle, which is usually plotted by normalizing the radiation intensity to its maximum value. The characteristics of the radiation pattern are determined by the aperture shape of the antenna and the current distribution on the aperture. Important parameters to present the radiation patterns are briefly described. The mainlobe expresses the maximum radiation direction that is opposite to the backlobe, and the other minor lobes are called sidelobes, which are separated by nulls where no radiations. The sidelobe level (SLL) means the amplitude of the peak sidelobe; the sidelobe just beside the mainlobe is called the first sidelobe. The front-to-back ratio (FBR) is the amplitude ratio of the peak mainlobe and the backlobe. The beamwidth, or more specifically, half power beamwidth (HPBW), is the angle subtended by the half-power points of the mainlobe.

The directivity D of an antenna is a measure of radiation intensity as a function of direction, i.e., the ratio of the radiation intensity in direction (θ, ϕ) to the mean radiation intensity in all directions, or to the radiation intensity of an isotropic antenna radiating the same total power. An approximate value of the D can be calculated in terms of the beam solid angle Ω, or the HPBW in the two orthogonal plane, i.e.,

$$D = \frac{4\pi}{\Omega} = \frac{4\pi}{\theta_{HPBW}\phi_{HPBW}} \cong \frac{41253}{\theta_{HPBW}\phi_{HPBW}} (\text{deg.}) \tag{2}$$

In general, the directivity without specifying a direction means the maximum value of the D. Most radars usually adopt the antenna with large aperture and high directivity. The relationship between the directivity and the power gain G are

$$G = D \cdot \eta_{eff} = \frac{4\pi A}{\lambda^2} \cdot \eta_{eff} = \frac{4\pi A_{eff}}{\lambda^2} \tag{3}$$

where A is the antenna aperture area, η_{eff} is the radiation efficiency of the aperture, and $A_{eff} = \eta_{eff}A$ is the effective aperture area. The power gain G is the product of directivity and radiation efficiency, which is the ratio of power radiated to power fed into the antenna. This is due to the antenna mismatch and transmission loss, which can be observed from the transmission line theory shown in Figure 1. The source impedance $Z_s = R_s + jX_s$ and the antenna impedance $Z_a = R_r + R_l + jX_a$ are complex conjugates so that the transmitter is matched to the antenna and the maximum power can be delivered to the antenna and radiated. Then the radiation efficiency can be expresses by

$$\eta_{eff} = \frac{R_r}{R_r + R_l} \tag{4}$$

Since the power source is connected to the antenna, as the load, through the transmission line (feed-line), the antenna has to be matched to the feed-line to effectively radiate the power into the space. If mismatched, the part of power will be reflected and form standing wave, which can be measured using the reflection coefficient Γ or the voltage standing wave ratio (VSWR):

$$\Gamma = \frac{Z_a - Z_s}{Z_a + Z_s};\ VSWR = \frac{1+|\Gamma|}{1-|\Gamma|} \tag{5}$$

The power radiated out is equivalent to the source power (P_s) minus the reflected power (P_{ref}) at the terminal of the antenna and feed-line, and the power dissipated at the antenna (P_l), i.e., $P_t = P_s - P_{ref} - P_l = P_s(1-|\Gamma|^2) - P_l$. In fact, the efficiency consists of reflection efficiency, conductor efficiency, and dielectric efficiency, so $\eta_{eff} = \eta_{ref} \times \eta_{cond} \times \eta_{di}$. For a well designed antenna, the conductor and dielectric efficiencies are close to 1 and the reflection efficiency is dependent on the impedance matching.

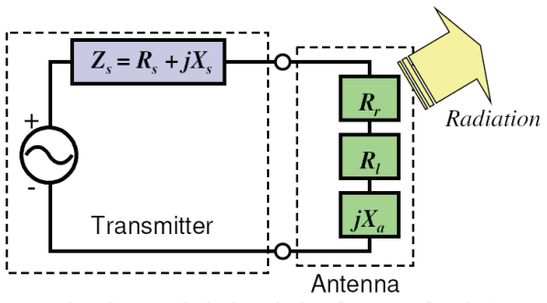

Fig. 1. Equivalent circuit of the transmitting antenna.

The polarization of an antenna can be determined by the electric field in the far-field region consisted of E_θ and E_ϕ. These two components will have a phase difference. When the phase difference is 0° or 180°, in the plane orthogonal to the propagation direction, these vectors oscillate in a straight line and this situation is called linearly polarized. When the phase difference is ±90°, it is called circularly polarized. For any other phase differences, it is generally called elliptically polarized. In practice, perfect circularly polarization does not exist, which means certain amount of ellipticity exists. This amount is expressed by the axial ratio (AR). Perfect circular polarization has AR = 1 (0 dB), and generally a circularly polarized antenna requires AR ≤ 3 dB.

2.2 Antenna array

Array antennas are often used in communication and radar systems to improve sensitivity and range extension without increasing power levels. Here, important design parameters for pattern synthesis and array scanning will be discussed. The configuration of the array antenna for different radar systems will be dressed and design considerations will be highlighted later.

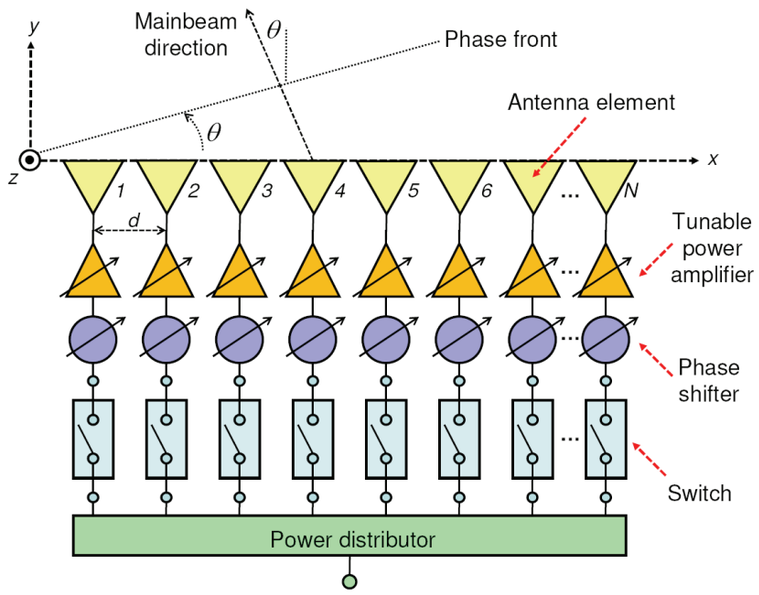

Fig. 2. Configuration of a linear array antenna.

A) Array pattern and grating lobe

The radiation pattern $F(\theta)$ of an array antenna is the product of the antenna element factor $F_e(\theta)$ and the array factor (AF) $F_a(\theta)$, i.e., $F(\theta) = F_e(\theta) \cdot F_a(\theta)$. The antenna element factor is the radiation pattern of a single antenna. To obtain the AF, we can start from the simplest array configuration, the linear array of N elements, as shown in Figure 2. The elements are separated in a distance d and it is assumed the phase reference is at the first element. The radiated field in far field from the array is given by

$$AF = \sum_{n=1}^{N} A_{n-1} exp(j(n-1)\psi) \tag{6}$$

with

$$\psi = kd\cos\theta + \beta \tag{7}$$

where $k = (2\pi/\lambda_0)$ is the wave number, θ is the arrival angle of the far-field, and β is the excitation phase for each element. The amplitude term A_{n-1} is used for the array amplitude taper that can be controlled by the tunable power amplifier; the phase term ψ is used for the phase taper that can be controlled by the phase shifter. If the phase reference is set at the center of the array that excited with a uniform amplitude equal to one, i.e., $A_n = 1$, the radiated field can be normalized as

$$AF_N = \frac{1}{N} \cdot \frac{1-e^{jN\psi}}{1-e^{j\psi}} = \frac{1}{N} \cdot \frac{\sin(N\psi/2)}{\sin(\psi/2)} \tag{8}$$

It can be observed that the pattern has peak vaule of 1 every 2π. The mainlobe at $\psi = 0$ is the mainbeam and the mainlobe at $\psi = \pm 2n\pi$ are the grating lobes. The grating lobe should be avoided becasue of receiving from unwanted directions. The condition to have the element spacing d satisfies

$$\frac{d}{\lambda} < \frac{1}{1+|\sin\theta_{0,\max}|} \tag{9}$$

where $\theta_{0,max}$ is the maximum directional angle that the mainbeam points to. The theory of the array scanning will be shortly described later. Here, let's consider the broadside array first which means the mainbeam is directed to boresight ($\theta_0 = 0^o$).

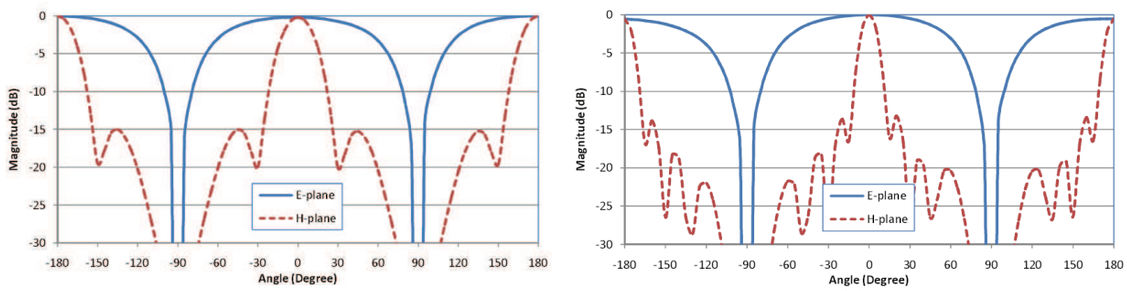

Fig. 3. Radiation patterns of a broadside uniform linear array with 8 elements: (a) $d = \lambda_0/4$ and (b) $d = \lambda_0/2$.

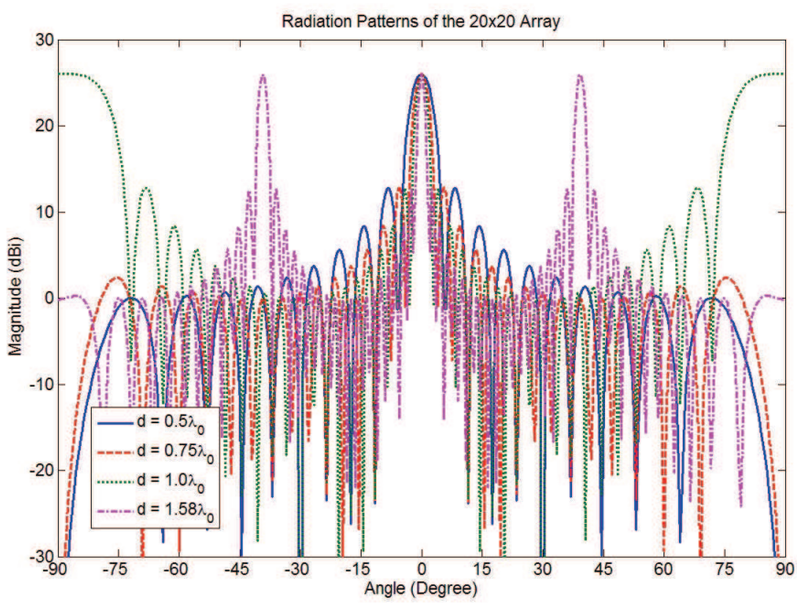

Fig. 4. Radiation patterns of a 20-element array with different element distances, while the mainbeam is at broadside direction.

A broadside array of N elements has a radiation pattern perpendicular to the array plane while the amplitude and the phase of each element are equal. In this case, Equation (7) can be reduced to

$$\psi = kd\cos\theta \tag{10}$$

Then the maximum field occurs at $\theta = \pi/2$ and $\theta = 3\pi/2$. Figure 3 shows the simulated radiation patterns of an 8-element broadside linear array with different element spacings, where the antenna element is an elliptical patch antenna. Comparing these two results, the patterns on the E-plane are almost the same. However, the H-plane pattern with $d = \lambda_0/2$ has a narrower HPBW compared to that with $d = \lambda_0/4$. As the element distance increases, the mainlobe become sharper but the grating lobe may appear which is not desired.

Figure 4 shows the radiation patterns with different element distances ($0.5\lambda_0$, $0.75\lambda_0$, $1\lambda_0$, and $1.58\lambda_0$), when the antenna elements is a microstrip patch antenna. When the mainbeam is at the broadside direction, the array with $d = 0.5\lambda_0$ does not have any grating lobe and the magnitude of grating lobes of the array with $d = 0.75\lambda_0$ are very small. However, when the spacing is larger than one wavelength, there are two obvious grating lobes. In the case of $d = 1.58\lambda_0$, the angle range between the mainbeam and the grating lobe is only 40^o, which significantly interference the desired signals.

B) Amplitude tapering and sidelobes

Array antennas can be employed in advanced radar systems to achieve the required power, high-resolution beam pattern, electronic beam steering, and interference suppression through nulling sidelobes. An array antenna can be excited by uniform or non-uniform amplitude taper, which can be implemented by using the tunable power amplifiers. As shown in Figure 2, all antenna elements can be turned on/off by the switch, which can decide how many elements to be used. Various combinations may happen, for example, eight or more elements could be used simultaneously as a sub-array. All of these elements are then connected to a power distributor, and then the summed signals can be processed and analyzed.

To implement a non-uniform amplitude taper for the array, several amplifiers are needed, as shown in Figure 2. In this case, assume all switches are turned on. To avoid the result of amplitude taper being obscured by grating lobe effects, the element spacing has to be equal to or less than half-wavelength. The easiest way to apply the amplitude taper is to linearly decrease the contribution of the array elements from the center to the edge of the array, which is called triangular amplitude taper. For an 8-element linear array, a triangular amplitude taper are given by: $A_1 = A_8 = 0.25$; $A_2 = A_7 = 0.5$; $A_3 = A_6 = 0.75$; $A_4 = A_5 = 1$. The uniform and triangular tapered radiation patterns of this broadside array with $d = \lambda_0/2$ are shown in Figure 5. It is observed that the triangular amplitude taper leads a lower SLL where the highest sidelobe is now −28 dB, compared to −13 dB of the uniform amplitude taper array. However, its mainbeam is broadened a little and increases from 12.8° to 16.4°.

It is possible to remove all sidelobes at the same time by using a proper amplitude taper such as the coefficients of a binomial series. The binominal amplitude taper for an 8-element is given by: $A_1 = A_8 = 0.03$; $A_2 = A_7 = 0.2$; $A_3 = A_6 = 0.6$; $A_4 = A_5 = 1$. Similar to the previous two cases, the resulting patterns are shown in Figure 5. While the sidelobes are suppressed, it can be seen that a more broadened mainbeam is the price of removing the sidelobes. In this case, the HPBW is about 22.2°.

In this example, it seems that using a linear method is the simplest approach for implementation in an array with only eight elements. However, as the element number increases, different non-uniform amplitude tapers should be chosen to narrow the mainlobe beamwidth or to suppress the sidelobe levels. Besides the binomial and trianular distributions, popular techniques for the amplitude tapering and sidelobe level control include circularly symmetric distribution, Bayliss Distribution, Hamming distribution, Hanning distribution, Chebyshev distribution, Taylor distribution, and Elliott distribution *et al* (Milligan, 2005).

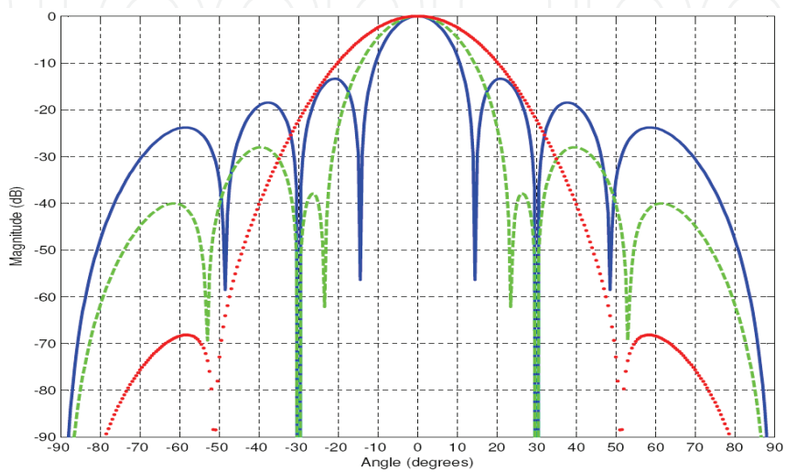

Fig. 5. Radiation patterns of an 8-element broadside linear array with different amplitude taperings. Solid line: uniform amplitude taper; dash line: triangular amplitude taper; dot line: binomial amplitude taper.

C) Phased array antenna

Based on the equation of the AF, if we want to direct the mainbeam of the array antenna to a desired direction θ_0, the AF will have the maximum value while ψ = 0 and hence $\beta = -kd\cos\theta_0$. Then the AF can be rewritten as:

$$AF = \sum_{n=1}^{N} A_{n-1} exp(j(n-1)kd(\sin\theta - \sin\theta_0)) \tag{11}$$

The concept of the linear array can be easily extended to the planar array such as rectangular array and circular array (Rudge *et al.*, 1983). Same as the linear array, the mainbeam of a planar array can scan toward any interested point. It is straight forward to have the AF of a *x*-*y* rectangular array directed to (θ_0, ϕ_0):

$$AF_{rec} = \sum_{m=1}^{M} A_m exp(j(m-1)kd_x(\sin\theta\cos\phi - \sin\theta_0\cos\phi_0)) \cdot \sum_{n=1}^{N} A_n exp(j(n-1)kd_y(\sin\theta\sin\phi - \sin\theta_0\sin\phi_0)) \tag{12}$$

Where A_m is the amplitude taper of the element in x-axis, A_n is the amplitude taper of the element in y-axis, d_x is the element spacing in x-axis, and d_y is the element spacing in y-axis. Figure 6 shows the radiation patterns of a 20×20 array with $d = 0.5\lambda_0$. It can be seen there is

no grating lobe even if the mainbeam is directed at 60°. As the scanning angle increases, the sidelobes close to ±90° becomes larger. However, they are still about 17 dB lower than the mainlobe. Therefore, from the view point of beamsteering, the element spacing, theoretically, has to be less than half wavelength if the mainbeam need scan to ±90°. In practical, we can have only ±60° scanning range at most, due to the degrading of the radiation patterns and the limitation of hardware.

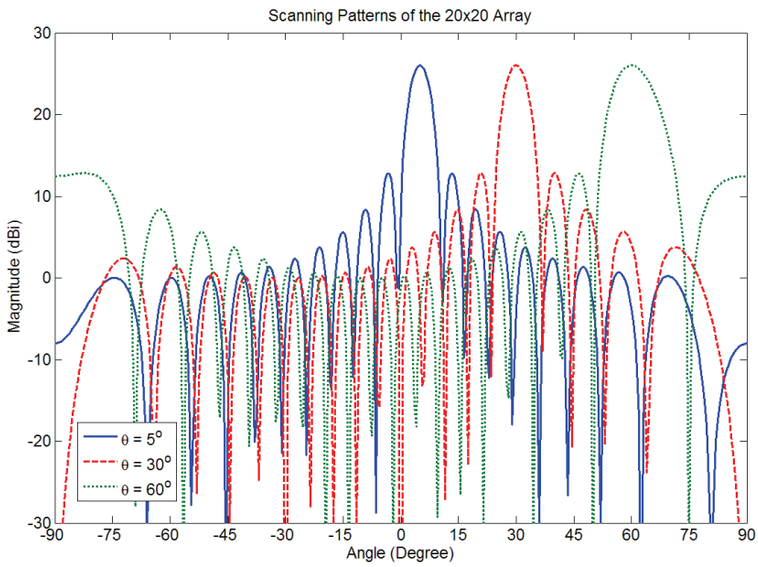

Fig. 6. Radiation patterns of a 20×20 array with different scanning angles, when $d = 0.5\lambda_0$.

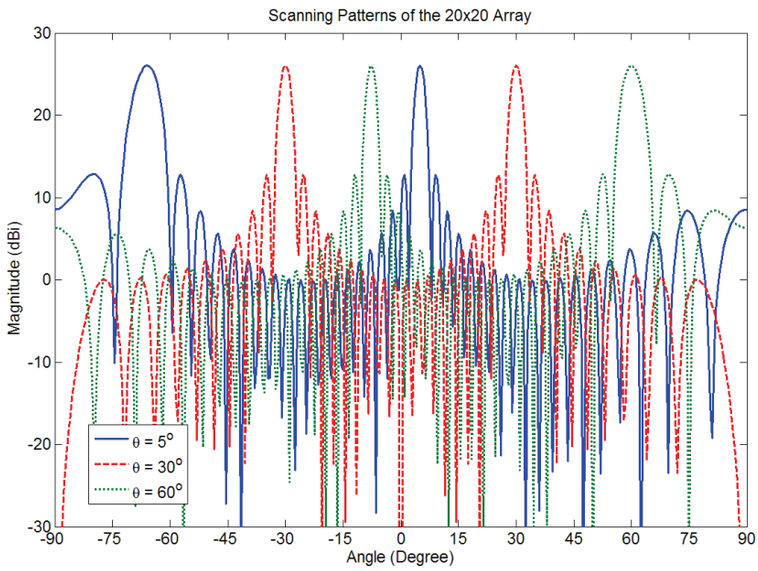

Fig. 7. Radiation patterns of a 20×20 array with different scanning angles, when $d = 1\lambda_0$.

Figure 7 shows the radiation patterns of $d = 1.05\lambda_0$, while the mainbeam is directed at different angles. Here radiation patterns of three scanning angles (θ = 5°, 30°, and 60°) are

shown. No matter how large angle the mainbeam scans, besides the mainlobe, there is at least one grating lobe directed at the unwanted direction. In Figure 4, it can be observed, when $d = 1.58\lambda_0$ there are two grating lobe when the mainbeam is at the broadside. The angle range between mainlobe and grating lobe decrease when the element spacing increases. From these results, it can be observed how the raidaiton pattern is affected by the element spacing.

There are many design considerations for the phased array antenna including mutual coupling and correlation, beam broadening, phase shifting, nulling undesired lobes, and feed network. Interested readers can review these topics in many published resources (Skolnik, 1990; Mailloux, 2005; Volakis *et al*, 2007). It should keep in mind that, from above discussion, to obtain a desired array pattern, we can vary: (1) array geometry, (2) array element spacing, (3) pattern of individual element, (4) element excitation amplitude, and (5) element excitation phase. After giving required array antenna characteristics, preliminary aperture and feed network designs will be conducted. Aperture distribution (amplitude taper) can be determined by aperture systhesis techniques, considering gain, beamwidth, sidelobe level, and etc. After optimization of the array antenna design, the fabrication and the testing can be implemented to verify the performance and readjust the design. The design process of an array antenna is shown in Figure 8. Based on these important concepts just reviewed, now we can look forward to see some antennas designed for different radar systems. In next section, we will look state-of-the-art radar antennas where their design concept and performance will be presented.

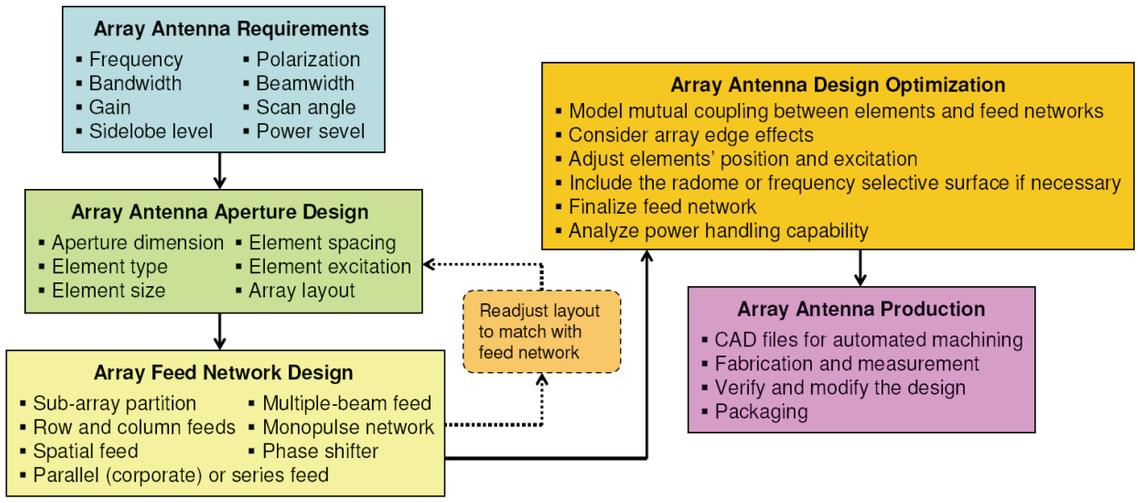

Fig. 8. Array antenna design process. One or more design iterations will be needed to achieve the design goal.

3. Radar antennas

3.1 Antennas for the airborne radar

Popular antennas for the ground-based and airborne radar systems include horn antennas, reflector antennas, and slotted waveguide antennas (Skolnik, 2001). These antennas can provide narrow beamwidth and high power handling. The airborne survillance radars and the air fighter radars usually need phased array antennas to conduct the beam steering for

the prupose of detection and tracking, which requires narrow mainbeam and very low sidelobes. The slotted waveguide antennas are better candidates for the large array antenna design because of the waveguide structure, which can couple energy in a very precise manner (low loss) and can be used for the feed network of the array antenna to simplify the phased array antenna design. The slotted waveguide array antennas (multiple slots on a single waveguide) have potential of low cost, low weight, ease of fabrication, high gain, and easier amplitude tapering for extremely low sidelobe. Today, they have been widely used in the airborne phased array radar systems.

The radiation magnitude and phase of the slotted waveguide antenna can be determined by the size and orientation angle of the slot. The apperance of grating lobes and the elemetn spacing govern the locations of slots. To optimze the bandwidth, the slots can resonate for either resonant array (standing wave array) or non-resonant array (traveling wave array). Basically, the radiation power is proportional to the slot resistance or conductance. Normalized series-slot resistance (r) and shunt-slot conductance (g) are given by

$$r = 2P/I^2;\ g = 2P/V^2 \tag{13}$$

where P is the required power; V and I are the voltage and current across the slot, respectively, which can be determined by the transmission line or scattering matrix theories, and hence r and g. Then, the slot array can be designed using on known, or measured, slot characteristics or design curves based on the slot geometry. Watson and Stevenson pioneered the slot characteristics for different slot geometries in a rectangular waveguide (Waston, 1949; Stevenson, 1948). Most of the closed form solutions can correctively predict the performance of the single slot. However, since the mutual coupling effect is neglected, the slot array based on these analyses will have higher VSWR and the aperture illumincation may not be the desired distribution. Several techniques have been proposed to overcome this difficulty (Volakis *et al*, 2007).

A) Resonant array (standing wave array)

The slotted waveguide array antenna cab be fed at edge or center with shorted port at the waveguide end. When the element spacing d_s is $\lambda_g/2$, the electrical fields inside the waveguide form standing waves, and hence the array antenna is called a standing wave array or resonant array. Figure 9 shows two types of the resonant arrays. Since the standing wave array is a narrow band antenna, to have the desired bandwidth, the slot number on each waveguide has to be analytically designed. Then, several subarrays, which consisted of several waveguides with different slot numbers, are shunt connected to form a planar array

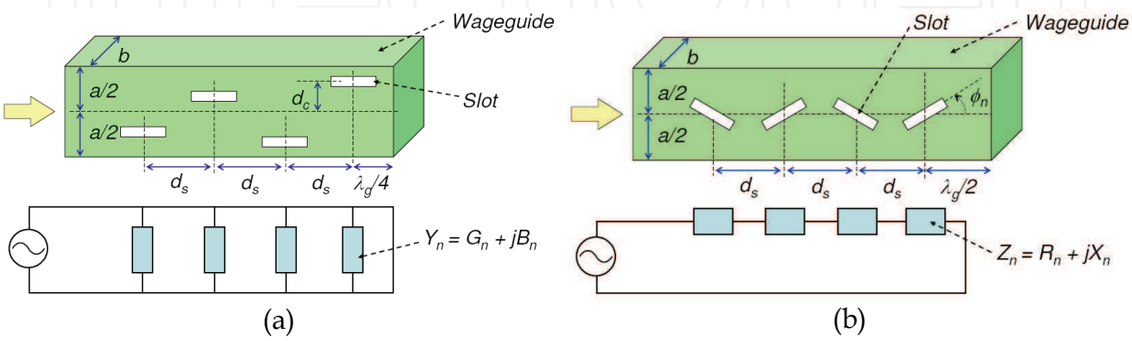

Fig. 9. The resonant slotted waveguide array antennas and their equivalent circuits using (a) shunt slots and (b) series slots.

that excited by another waveguide coupling the energy to the subarrays. Generally, the more slots on a waveguide, the narrower bandwidth. When the operation frequency offsets from the designed center frequency, the gian decreases and the SLL increases, due to the change of the electric field (standing wave) distributions in the waveguide that deteriorate the amplitude and phase excited. Large planar arrays of uniformly spaced longitudinal-shunt-slots are commonly used for many airborne radar applications.

B) Non-resonant array (traveling wave array)

The traveling wave array is fed from one port of the waveguide and the other port connects a matched load to terminate the waveguide that absorbing energy not radiated. The non-resonant array has more slots on each waveguide than the resonant array. The element spacing of this array is not eqaul to $\lambda_g/2$ (may be larger or smaller) to avoid reflection, so the reflected wave from each slot do not generate large standing wave due to constructively field accumulation. The reflected power from the termination has to keep sufficiently small so the spuriois beam is below the required SLL. Also, becasuse of unequal element spacing, there are phase differences between slot elements, which results in the mainbeam deviates the broadside direction and changes with the operation frequencies.

C) Frequency scanning array

One of the important applications of the slotted waveguide array antenna is to design the frequency scaning array (FSA) antenna, which is a kind of electrically scanning array by controlling the operation frequencies. Frequency scanning array have two feeding meethods: series-fed and cooperated-fed. It usually uses slow wave to feed the slotted waveguide. The feed line network of a linear FSA can be analyzed in equivalent slow wave structure, whose phase speed (v_p) is

$$v_p = \frac{d}{L} \cdot \frac{\lambda_g}{\lambda_0} \cdot c \tag{14}$$

Where L is the length difference of the feed-lines for neighboring elements, c is the light speed, and λ_g is the wavelength in the waveguide, which is given by

$$\lambda_g = \frac{\lambda_0}{\sqrt{1-(\lambda_0/\lambda_{cf})^2}} = \frac{\lambda_0}{\sqrt{1-(\lambda_0/2a)^2}} \tag{15}$$

λ_{cf} is the cutoff wavelength of the waveguide, which is equal to twice of the waveguide width ($2a$). Assume the frequency scanning occurs relative to a desired center frequency (f_s). From the far-field pattern of the slotted waveguide array, it can be shown that the maximum pattern exists while

$$\frac{2\pi}{\lambda_0} d \sin(\psi_m) + \pi - \delta = 2m\pi, m = 0, \pm 1, \pm 2, ..., \tag{16}$$

$\delta = 2\pi d/\lambda_g$ is the phase difference between slot elements. Using the condition of broadside ($\psi_m = 0$) at the center frequency and Equation (15), we can derivate

$$\sin(\psi_m) = \sqrt{1-(\frac{f_{cf}}{f})^2} - \frac{\lambda_0}{\lambda_g} \cdot \frac{\lambda_0}{\lambda_s} \tag{17}$$

Now, let $f_{cf} = \kappa \cdot f_s$, then this equation can be re-written as

$$\sin(\psi_m) = \sqrt{1-\kappa^2 (\frac{f_s}{f})^2} - \sqrt{1-\kappa^2} \cdot \frac{f_s}{f} \tag{18}$$

This equation gives the relationship between these frequencies and how to scan the mainbeam by tuning the operation frequency for the slotted waveguide array. In fact, the scanning angle with frequency is rather confined, due to the fixed path length limited by the waveguide configuration. If a larger scanning angle is required, the waveguide can be bent to lengthen the path. However, this will change the feeding structure and waveguide configuration, and results in larger volumn and higher cost.

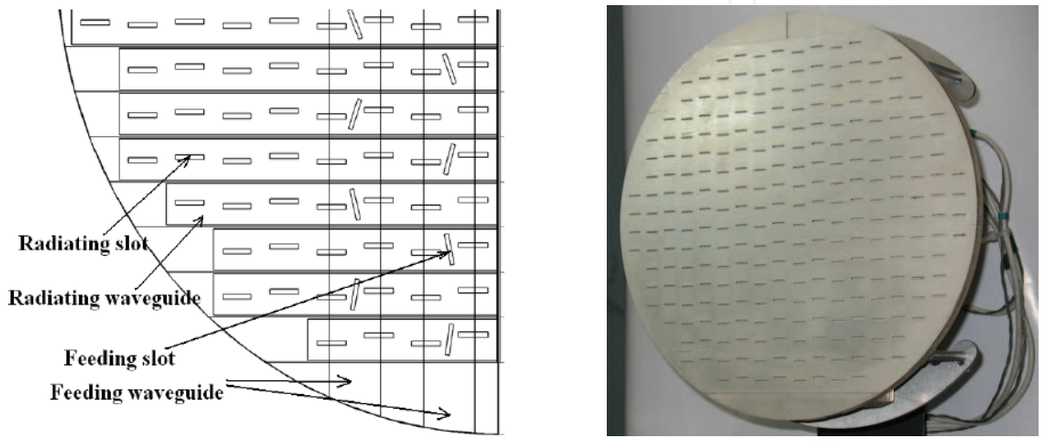

Fig. 10. A circular slotted waveguide array antenna: (a) antenna configuration and (b) antenna photo.

The frequency scanning array antenna can support 3-D scanning while it uses mechanical scan in the azimuth plane and electrical scan in the elevation plane. The advantages include small volume, light weight, and good mobility. Several engineering concepts should be considered to evaluate the phased array antenna performance:

1. To satisdy the requirements of broadband and low sidelobe, the traveling wave arrays using the rectangular waveguide are generally adopted.
2. To suppress the cross-polarization of the planar array, the inclined angles between waveguides should be in the opposite direction. The phase of the excitation source for each waveguide needs be carefully designed.
3. To lower the weight of the waveguide, the materials with low specific gravity can be used.
4. While electrically scanning in the elevation plane, the feeding waveguide forms an array in the azimuth plane so the mainbeam in the azimuth plane will be affected. This angle deviation has to be corrected to avoid detection error.
5. The temperature variaion due to the envioronment or the materials heated by the radiation power will result in the mainbeam direction shift and thus has to be considered for high power applicaitons.

Besides, some of the second-order effects such as the slot alternating displacement, inclined angle alternation, edge effects, non-uniform aperture illumination, slot length error, and

mutual coupling through the high-order modes would degrade the array performance than what expected. Manufacturing tolerance also affects the accuracy of the array. These parameters should not be ignored in the phased array antenna design. It is normally to overdesign the array antenna for analysis and fabrication deficiencies that would rely on experience. Figure 10 shows a Ku-band slotted waveguide array antenna for airborne radar applications (Sekretarov & Vavriv, 2008).

3.2 Antennas for the ground penetrating radar

Ground-penetrating radar (GPR) is a geophysical method that uses radar to image the subsurface. This non-destructive method uses electromagnetic radiation in the microwave band (3-30 GHz) of the radio spectrum, and detects the reflected signals from subsurface structures. GPRs can be used in a variety of media, including rock, soil, ice, fresh water, pavements and structures. It can detect objects, changes in material, and voids and cracks. Landmine detection is also an emergent application for GPRs. Unfortunately, there is little international effort to detect and clear the landmines due to shortage of funding. Before they can be removed, they must be located and the ultra-wideband (UWB) GPR technology is ideal for finding the location of these deadly devices. Here we present the antennas popularly used in the GPR applications, which can provide desired bandwidth.

A) TEM horn antenna

For air-launched GPR systems, TEM horn antenna is a good choice because it meets the demand in the aspects of a wide bandwidth, small distortion, directional radiation pattern, and small reflection. It is usually made from two tapered metal plates, including exponentially tapered or linearly tapered. There are a narrow feed point and a wide open end at both sides of the TEM horn antenna (Milligan, 2004). Figure 11 shows a TEM horn antenna which is most widely-used as the GPR antenna (Chung & Lee, 2008).

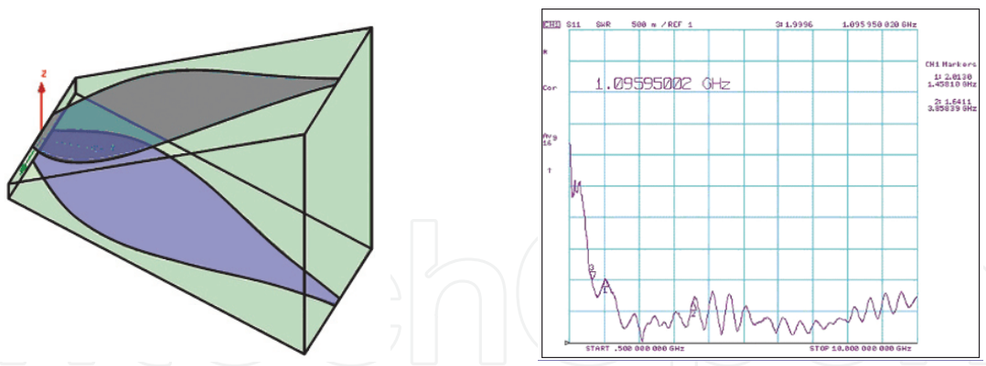

Fig. 11. A TEM horn antenna which can cover 1-10 GHz (VSWR < 2).

B) Monopole antennas

Plenty modifications of monopole antennas are used for broadband applications. The cone antenna is a typical representative, which is usually made as three dimensional structures with a direct coaxial feeding, as shown in Figure 12. The basic electric property of elementary monopole antennas is linearly polarized omni-directional radiation, which changes to a common one with increasing frequency. From this reason, these antennas are used especially in mobile terminals. Typical fractional impedance bandwidth of the monopole antenna is about 70-80%. Further improvements can be made by means of forming the ground plane shape.

The development of high-frequency substrates has enabled the planar design of the monopole antennas. Planar monopole antennas are made single-sided, fed by a coplanar waveguide (CPW), or dual-sided with a microstrip feed line. An example is shown in Figure 13. The advantages are in a manufacture and in an occupied space. However, it is noted that antennas on the planar substrate may have lower radiation efficiency/gain.

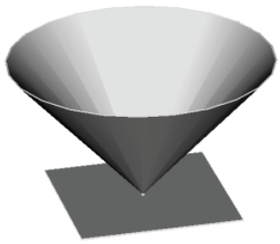

Fig. 12. Cone antenna.

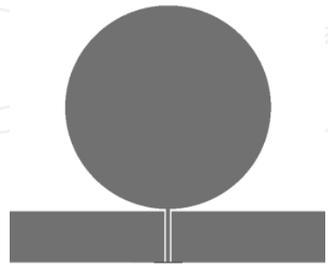

Fig. 13. Planar CPW-fed monopole antenna.

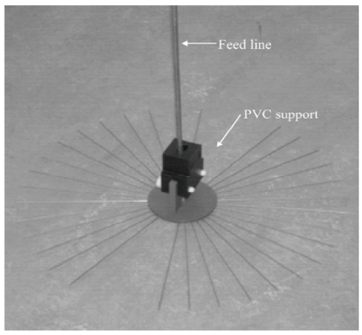

(a)

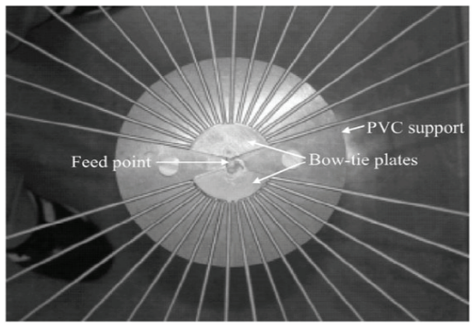

(b)

Fig. 14. (a) Experimental adaptive wire bow-tie antenna and (b) its feed region. The wires are hold together by a PVC support.

It has been known that when an antenna is situated in a proximity to the ground, its input impedance varies significantly with the antenna elevation and the type of the ground. From the system point of view, such input impedance variation is disadvantageous since it leads to difficulty in maintaining a matched condition at the antenna's terminal. When the maximum power transferring from the transmitter to the antenna, via a transmission line, is considered critical, one should provide a variable matching device which is capable of coping with such impedance variation to achieve a matched termination of the antenna for different antenna elevations and ground types. The new design of the GPR antenna allows such a fast and convenient way for controlling the bow-tie flare angle required in a real GPR survey, while the antenna could promptly adapt to any changes in antenna elevation and soil type, as shown in Figure 14 (Lestari *et al.*, 2005).

3.3 Antennas for the noise radar

Wideband random noise radar technology works by transmitting a random noise waveform and cross-correlating the reflected echoes with a time-delayed (to obtain range information) and frequency-shifted (to ensure phase coherence) replica of the transmit signal. Random noise signals are inherently difficult to detect and jam. Since signal reflected from the target

is compared with reference from noise generator. Any distortions added to the reflected signal from the target to receiver will have an influence on radar properties, for example, accuracy of target position measurement or resolution of the target. One of the important elements of distortions is antenna. Noise radars usually have separated antennas for transmit and receive due to the need of good cross-coupling isolations. Specific features of noise radars causes that requirements for its antenna systems are similar to other wideband radars.

Some types of antennas are especially compatible with requirements for wideband noise radars, including horn antennas, notch antennas, log-periodic antennas and spiral antennas. The common properties of those antennas are their wide bandwidth. However, most of the noise radar systems will need high gain and high directivity to increase the probability of detection for the short-distance target which is less than 200 meter in front of the radar. The noise radars usually require CW amplifier which has its limitation of maximum transmit power. High gain (> 7 dBi) and wideband antennas are always preferred.

Below there are presented the most popular antennas for wideband applications with described their main properties from the point of view of the noise radar systems. The distortions introduced to the system by antennas can be divided in two main parts: amplitude and phase distortions. The amplitude distortions are caused mainly by antenna gain fluctuations or VSWR properties. In case of phase distortions the main reason are dispersive properties of the antenna. Only non-dispersive antennas are free of that problem (Wisniewski, 2006).

A) Ridged horn antenna

To extend the maximum bandwidth of horn antennas, ridges are introduced in the flared part of the antenna. This is commonly implemented in waveguides to decrease the cutoff frequency of the dominant propagating mode and thus expands the fundamental mode range before high-order modes occur (Hopfer, 1955; Chen, 1957). While the bandwidth of a standard horn is typically up to 2:1, the bandwidth of ridged horns can be up to 18:1. One ridged horn antnena is shown in Figure 15. The ridged horn antenna has high gain directional pattern and shaped radiation pattern in both planes. It can be linear (double-ridge) or dual-polarized (quard-ridged) and dispersive that depend on the ridge design. The main application for noise radars lies in ground penetrating, foliage penetrating, SAR imaging, and tracking.

B) Log-periodic antenna

One good candidate for the noise radar availiable in the market is the Log-Periodic Yagi antenna, as shown in Figure 16. From our radar experiment (Lai & Narayanan, 2005), it was found that this antenna has very good performance over UHF frequency band (400–1000 MHz). It can provide an extended bandwidth of 50 MHz beyond the mentioned lower cutoff frequency of the antenna. Their maintenance free construction on rugged FR-4 material boasts of the added advantages of tuning-free, non-fragile antenna elements. The small size and wide bandwidth makes them ideal for feeding reflector antennas such as the easily constructed corner reflectors or parabolic grids. This antenna also features an SMA Female connector, and their wide bandwidth characteristic ensures total reliability within their respective ranges.

C) Spiral antennas

The bandwidth of spiral antennas is even up to 40:1 and directional in both E- and H-planes. Beamwidth has small changes along with frequency changes. It is usually circular polarized and dispersive. Possibility of application is for noise radar antenna arrays and penetrating detection. More information about the spiral antennas will be presented in next section.

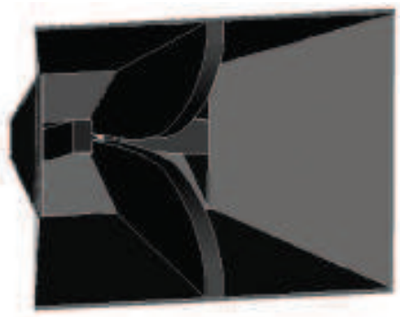

Fig. 15. Construction of the ridged horn antenna

Fig. 16. Planar log-periodic antenna

3.4 Antennas for the UWB system

The development of the ultra-wideband (UWB) sources and antennas has been significantly progressed. UWB antennas need a constant phase center and low VSWR across the whole operation bandwidth. A change in phase center may result in distortion of the transmitted signals and worse performance at the receiver. Hence, UWB antenna design is one of primary challenges in the design of UWB radar systems, especially when low-cost, geometrically small, and radio-efficient structures are required for typical radar applications. It is difficult to compare a UWB antenna with a conventional antenna because the performance considerations for the conventional antenna are based on continuous wave or narrowband theory. However, basic concepts for antenna design should be kept in mind when a conventional approach is used for UWB antennas (Allen *et al.*, 2007).

In the UWB antenna desing, perhaps the most significantly question is: what kind of structures result in ultra-wideband radiation? It has been knonw that several mechanisms can give such a wide bandwidth, and their combinations would be an alternative way to implement (Wiesbeck *et al.*, 2009). These includes: 1) frequency independent antennas (the antenna shape is in terms of angles); 2) self-complementary antennas; 3) traveling-wave antennas; 4) multiple resonance antennas. However, none of anyone structure can guarantee constant radiation patterns over the whole bandwidth. In most cases, the radiation patterns distort from the omni-directional pattern or dipole-like pattern as the operation frequency increases. Also, current commercial UWB systems with impulse signals is seeking for compact antenna solution so that the antenna can be easily packaged with the transceiver module. Therefore, it is obviuosly that the design of UWB antennas should consider the following requirements. First, the bandwidth of the antenna has to satisfy the specification and not interfere the frequency bands used by other wireless systems. Recently, many frequency-notched UWB antennas have been reported to avoiding the conflict between the ISM band. Secondly, the size of the antenna should be miniaturized and compatible to the UWB unit. Thirdly, the UWB antenna should have a omni-directional coverage, indepent of the frequency. Forthly, the antenna would require good time-domain characteristics subjected to the UWB system specification. In this seciton, we will introduce two UWB antennas with the performance qualified the requirements mentioned above.

A) Coupled sectorial loop antenna

The coupled sectorial loop antenna (CSLA) is designed based on the magnetic coupling of two adjacent sectorial loop antennas in a symmetric geometry (Behdad & Sarabandi, 2005). Figure 17(a) shows the topology of a coupled loop antenna arrangement. Two loop antennas

(Antenna 1 and Antenna 2) are placed in close proximity of one another. The antennas are located in the near field of each other and thus a strong mutual coupling between them exists. This mutual coupling can be controlled by changing the separation distance between the two loops and the shape of the loops. If the two antennas are fed with a single source in parallel at the feed location, then

$$Z_{in} = (Z_{11} + Z_{12})/2 \tag{19}$$

where Z_{in} is the input impedance of the double-element antenna, Z_{11} is the self impedance of each loop in the presence of the other one and Z_{12} is the mutual coupling between the two loop. The self impedance of each loop (Z_{11}) is mainly a function of its geometrical dimensions and does not strongly depend on the location and separation distance of the other loop. On the other hand, the mutual coupling (Z_{12}) is mainly a function of separation distance between the two loops as well as the geometrical parameters of each loop. It is possible to choose the dimensions of each loop and the separation distance between the two loops in a manner such that the variations of Z_{11} vs. frequency cancel the variations of Z_{12}. Consequently, a relatively broadband constant input impedance as a function of frequency can be obtained.

Since the antenna topology shown in Figure 17(a) needs a balanced feed, a coaxial cable is used to fed half of the antenna along the plane of zero potential (z = 0) over a ground plane, as shown in Figure 17(b). The CSLA is printed on a dielectric substrate of 3 cm × 1.5 cm,

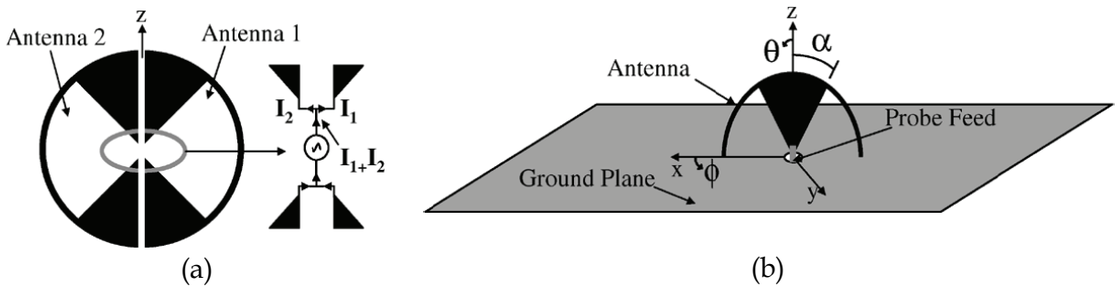

(a) (b)

Fig. 17. (a) Topology of the CSLA; (b) Half of the CSLA is used, which is balanced fed by a coaxial probe.

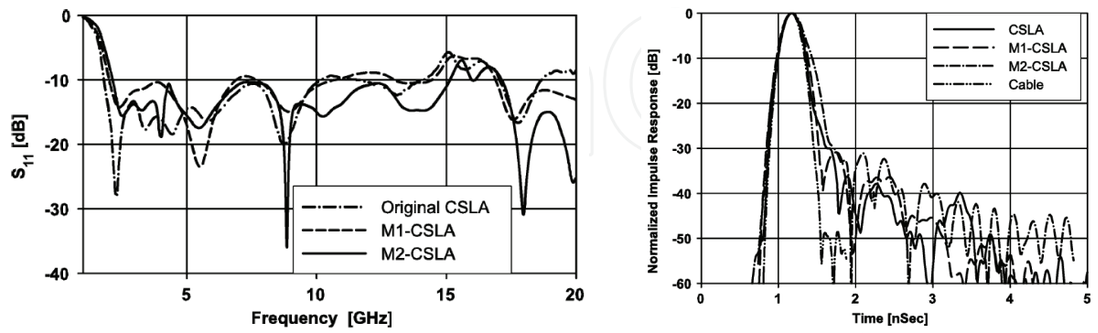

(a) (b)

Fig. 18. (a) Measured return losses of the CSLAs. The original CLSA is shown in Fig. 17(b). M1-CSLA and M2-CSLA are the modifed CLSAs with controlled arch angle or notched metal radiator (topologies not shown); (b) time-domain impulse response using two identical CLSAs.

with a relative dielectric constant of 3.4 and thickness of 0.5 mm, and the ground plane size is 10 cm × 10 cm. The self and mutual impedance of the CSLA can be changed by changing the antenna dimensions including the arch angle, α, which gives an additional degree of flexibility in shaping the frequency response. It has been shown that this compact topology can provide an impedance bandwidth in excess of 10:1, as shown in Figure 18(a). Figure 18(b) shows the normalized time-domain impulse responses using two identical CLSAs, which are very close to that of the coaxial cable with the same electrical length. Figure 19 shows the azimuthal radiation patterns and these remains similar up to 8 GHz. They start to change as the frequency is higher than 10 GHz. The gain of this antenna is between -5 dBi to +4 dBi when the operation frequency is lower than 10 GHz.

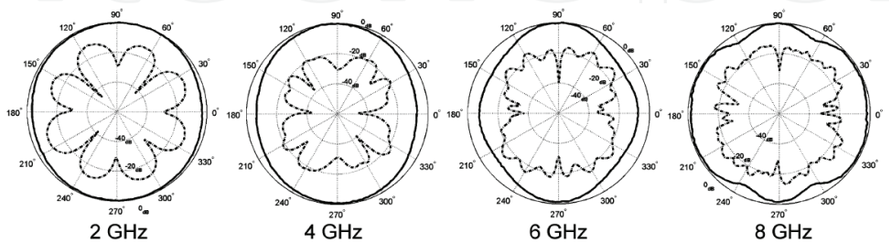

Fig. 19. Measured radiation patterns in the azimuth plane. The solid line and the dash line are co-polarized (E_θ) and cross-polarized (E_ϕ) components, respectively.

B) Frequency independent antenna

An UWB antenna that is able to cover the lower frequency bands such as HF-UHF is challenging due to the requirement and limitation of the bandwidth and physical-size. The spiral antenna is a frequency independent antenna and is a good candidate for UHF and below applications. To have a broadband operation frequency, the integration of multi-arm spiral antennas with broadband balun and feed structures can present numerous challenges. Many innovative designs have been implemented that provide the broadband differential excitation to the complimentary arms of the spiral. In these designs, the Dyson balun provides a very compact form that can be integrated into the structure of the antenna. However, since this balun's implementation typically involves coaxial line, its implementation can create difficulties within the context of IC fabrication techniques. Thus, a design that integrates the spiral antenna, balun, and feed network into a multi-layer structure can provide many possibilities, including antenna miniaturization and bandwidth maximization.

The design of spiral antennas has four primary components: (1) the geometry of antenna, (2) the finite-ground stripline structure, (3) a stripline impedance transformer, and (4) the balun. The spiral antenna is created by winding the finite-ground stripline structure into one arm of the spiral, and extending the center-conductor through the middle of the spiral (the balun) into the complimentary arm of the spiral. The stripline grounds in this configuration will act as both a part of the feed structure and a distributed arm of the spiral antenna. The impedance transformer can then be positioned along the feed section into the center of the spiral to provide the impedance match.

The spiral antenna properties and performance of the finite-ground stripline will have an intimate relationship based around the arm-width constant K (or slot-to-metal ratio). This parameter impacts the input impedance and radiated fields of the spiral, but can also be treated as a degree of freedom between the spiral and stripline geometries. For the finite-

ground stripline, this parameter will impact the guiding properties and effectively create a lower bound for its characteristic impedance. Therefore, the parameter *K* can be used to create a spiral with an input impedance that corresponds to a desired width of the stripline center-conductor for both guidance and obtaining an impedance match with the spiral antenna. By using a high impedance line that corresponds to a narrower line width, small feature sizes can be created. The use of an impedance transformer along the winding of spiral will match the input impedance of the spiral with the system impedance.

An Archimedean spiral with a slot-to-metal ratio of 0.75 has been designed on Rochelle foam for the experimental validation of the stripline-based spiral antenna design using Dyson-style balun (Huff & Roach, 2007). The antenna is designed to operate from 800 MHz to 4.5 GHz. Figure 20 shows the spiral geometry with the simulated input impedance and VSWR. Note that this spiral only has single turn. With more turns, the lowest operation frequency of the antenna can be decreased. Theoretically, the effective frequency of the spiral should not have an upper limit.

The radiation pattern of the spiral antenna is stable within the whole operation frequencies due to its constant proportionality ratio, as shown in Figure 21. The planar spiral antenna exhibits a bidirectional radiation property. By placing a cavity-backed absorbing material, or using a ground plane, behind the antenna, the antenna will have a unidirectional pattern. This constant pattern characteristic avoids the use of beamforming for certain incident angles and reduces the attenuation due to the multi-paths. Considering the role of the mobile platform where the antenna installed, it can behave as a special reflector to

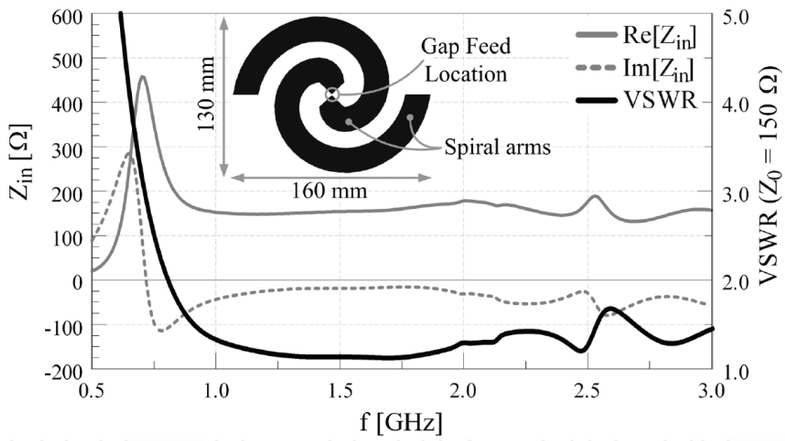

Fig. 20. Geometry of the spiral antenna, with its simulated input impedance and VSWR.

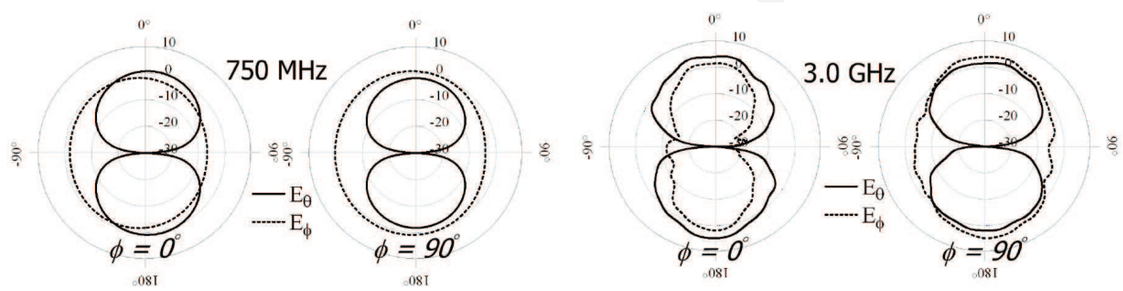

Fig. 21. Measured radiation patterns of the fabricated spiral antenna.

constructively add signals in phase and hence strengthen the radiation gain, which can increase the efficiency of the radio link and decrease power consumption to amplify the transmitted or received signals. Also, the spiral antenna can be used to from a high gain array by using a well-designed impedance matching network.

C) Polarization and antenna miniaturization

In some wireless applications, circular polarization is preferred to linear polarization due to the following reasons. First, while using a linear polarized antenna, the strength of the reflected signal from an object will depend on the azimuthal position of the antenna relative to the object. Secondly, if the direction of the transmitting antenna and the receiving antenna is orthogonal, the receiving antenna cannot detect the reflected signal from the object. Broadband dipole antennas, log-periodic antennas, and Yagi-Uda antennas are linear polarized broadband antennas and broadband circular polarization is relatively difficult to implement, compared to realize the circular polarization of spiral antennas.

Since the physical size of the low frequency antenna would be very large, the antenna miniaturization should be considered. The resonant frequency of the antenna can be reduced by using pieces of dielectric material to sandwich the antenna. In other words, it is also possible to reduce the size of the antenna at a given resonant frequency. On the other hand, both the thickness and permittivity of the substrate influence the antenna performance. A thick substrate with a low dielectric constant provides better efficiency and wider bandwidth at the expense of larger antenna element size. The same result can be obtained using a thin substrate with a high dielectric constant. Therefore, there is a trade-off between the efficiency and the physical size of a designed structure.

4. Antenna protection and filtering

4.1 Radome

For radar applications, a radome (a contraction of radar and dome) capable of protecting the antenna from the effect due to harsh environmental and other physical conditions must be developed. The radome should be capable of shielding the antenna from various hazardous conditions and not adversely affect the performance of the antenna. Therefore, investigation of the antenna protecting issue is an important task that must be carried out concurrently with development of the radar systems.

The antenna radome has many important parameters to be considered. Firstly, it has to withstand specified vibration, shock, and acceleration levels, including explosion and gunfire. In general, the radome may be used in the following scenarios:

1. For the ground use, it works form -50^{o}C to 60^{o}C, with relative humidity of 0-95%. It can not be damaged in wind speed of 67m/s and can afford ice/hail/snow load by 300 kg/m^2 at least.
2. For the airborne use, it works from -50^{o}C to 70^{o}C, with relative humidity of 0-95%. The altitude ranges from 0 to 12,000 meter.
3. For air fighter, the requirement is harder. The temperature is -50^{o}C to 180^{o}C and the altitude is 0-20,000 meter.

Besides, it has to be resistant for rain adhesion, rain erosion, and hail impact, should be fire retardant and lightening-protected, and is able to withstand solar radiation and even damage from nuclear explosions, if applicable.

The parameters list below can be used to evaluate the performance of the radome after integrated with the antenna:

1. Transmission and reflection coefficients: determines how much energy may loss or be reflected from surfaces, both internal and external diffraction and refraction effects.
2. Half-power beamwidth of the antenna: affects the coverage range and resolution.
3. Error in broadside: the mainbeam of the antenna may deviate from the broadside direction.
4. Pattern distortion and sidelobe change: the mainbeam shape of the antenna may change and the sidelobe level of the antenna may becomes worse. Also, the reflection due to the radome may result in new sidelobes.
5. Cross-polarized isolation: the cross-polarized pattern of the antenna may change, and the cross-polarized isolation may be enhanced/degraded.
6. Scanning error: the scanning range may be changed.

Several kinds of wall contruction have been used in radomes such as homogeneous single-layer (monolithic), multilayer and metallic-layer:

1. Monolithic wall includes thin wall and half-wave wall, which consists of a single slab whose thickness is less than $0.1\lambda_0/(\varepsilon_r)^{0.5}$ (thin wall), or is an multiple of half-wavelength ($n\lambda_0/2$), where n is the order of the radome wall. More strictly, the thickness of the monolithic wall is given by

$$t = \frac{n\lambda}{2} \cdot \frac{1}{\sqrt{\varepsilon_r - (\sin\theta)^2}} \tag{20}$$

   The thin wall can provide good electrical property, adequate strength, and regidity. However, it can be structrally weak. The half-wave wall should have no reflection at its incidence angle θ and thus the energy can be transmitted with minimal loss within a range of incidence angle. The ohmic loss is the primary loss of such material.
2. Multilayer wall includes A-sandwich, B-sandwish, C-sandwich, and the sandwich with even more layers. The A-sandwich have two thin, high-dielectric skins seperated by a low-dielectric core material of foam or honeycomb. The B-sandwich is a inverse version of the A-sandwich whose core is a high-dielectric skin. The C-sandwich consists of two back-to-back A-sandwichs for greater strength and rigidity.
3. Metallic radome can provide the necessary frequency filtering, which can be combined with the dielectric radomes. Conducting metal material with features of periodic patterns can be designed to have the characteristics of the lumped element shunted across a transmission line (thin layer), or of the waveguide with cuf-off frequency. Such elements can results in a planar or conformal frequency selective surface (FSS), which will be introduced in next section. Metallic radomes have better potential for higher power handling, suppressed signal interference, reduced static charge buildup, and strong resistance to rigid weather such as heat, rain, and sand.

It is expected that the use of radomes should have the following goals and advantages for the antenna operation: (a) the antenna can work in all-weather operation, (b) a cheaper antenna is produced because it requires less maintenance, (c) the overall system performance may be more accurate and reliable, and (d) the structural load of the antenna is reduced due to the removal of environmental forces. In terms of the fabrication process and tolerance, the radome has to be designed and optimized concurrently with the platform

geometry and critical design parameters for the antenna systems. Furthermore, through the radome to reduce the antenna RCS is an efficient way to protect the antenna and extend it lifetime, because the antenna may be detected and attacked by the enemy. More information of the performance analysis and materials for radomes can be found in (Rudge *et al.*, 1983; Kozakoff, 1997; Skolnik, 2001).

4.2 Frequency selective surface

A frequency selective surface (FSS) is a periodic surface that exhibits different transmission and reflection properties as a function of frequency. Two basic types are the array of wires (dipoles) and the array of slots, which are followed by a dielectric slab to form the FSS. As shown in Figure 22, an array of resonant dipoles acts as a spatial bandstop filter; an array of slots acts a spatial bandpass filter. However, unlike microwave filters, the frequency response of an FSS is not only a function of frequency but also a function of the polarization and incidence angle. In general, a FSS can be designed based on the transmission line theory to predict the desired transmission characteristics.

Figure 23 shows a newly developed low profile muti-layer FSS (Behdad *et al.*, 2009), which applied the third-order bandpass frequency response, with an overall thickness of only $\lambda/24$. Each layer is a two-dimensional periodic structure with sub-wavelength unit cell dimensions and periodicity, where both resonant and non-resonant elements have been combined and miniaturized. It also shows that the multi-layer FSS can be analyzed using the transmission line model to calculate required parameters for the periodic structures. This new design demonstrates a rather stable frequency response as a function of the incidence angle without the aid of any dielectric superstrates that are commonly used to stabilize the frequency response of FSS's for oblique incidence. The polarization has to be considered in the FSS deisng. Various periodic structures and unit elements have been proposed for single- and dual-polarized FSS's (Wu, 1995; Munk, 2000).

Besides, to minimize the size and weight of the FSS structures, high-dielectric ceramic materials can be used. Dielectric breakdown measurement could be first performed at macro-level to give the guideline on the FSS element designs. When properly designed, these ceramic materials are capable of reducing significantly the size of the FSS element and can handle high-power energy. To understand the microscopic structures of materials, mixing-law can be used to obtain microscopic-level field distribution within the materials that help further understand the dielectric breakdown mechanism. In addition, by mixing

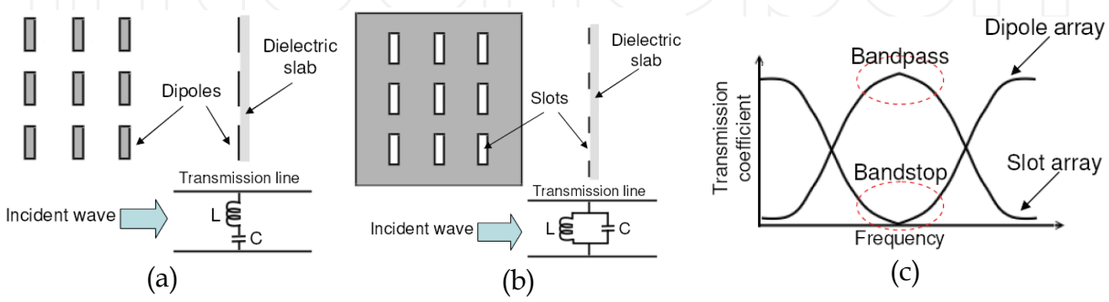

Fig. 22. Basic frequency selective surfaces: (a) dipole array, (b) slot array, and (c) frequency responses.

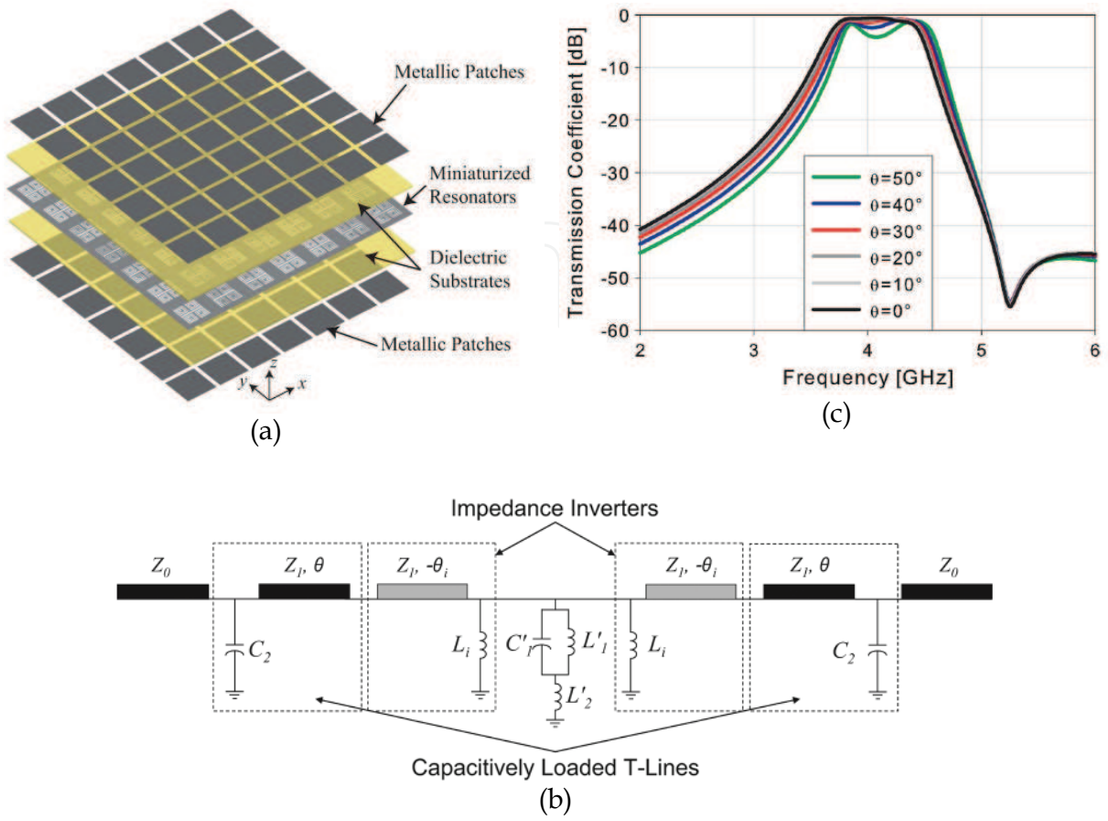

Fig. 23. A multi-layer third-order FSS: (a) topology, (b) equivalent circuit, (c) measured transmission coefficients for various incidence angles.

materials of two or more different dielectrics, synthetic dielectrics with different textured substrates can be developed for impedance matching. Combining all of these characteristics with the FSS configuration, it is possible to improve upon past benchmarks of bandwidth and power handling while maintaining significant miniaturization.

FSS's can be used to limit electromagnetic interference (EMI) and radar cross section (RCS) associated with antennas. When designing high power microwave (HPM) systems, problems associated with air and material breakdown must be addressed. However, at the present time, many advanced materials, including FSS's, are not employed in HPM systems due to breakdown concerns. The major reason for this is that both the macro-level electric field distribution within FSS unit element and the micro-level electric field distribution within dielectric materials have to be modeled simultaneously. For example, even two composite dielectric materials may have the same dielectric constant, due to the internal microscopic level construction, the breakdown voltages of these materials can be significantly different. Innovative designs are needed to allow FSS's to be employed in HPM systems. In addition to the power handling capability, other performance parameters, such as resonant frequencies and bandwidth, as well as compactness of FSS structure are also important. Good methodology to predict, test, and validate the power handling capability of FSS designs are hence highly desired for future FSS applications.

5. Conclusion

In this chapter, the basics of the antenna and phased array are reviewed and different wideband antennas for modern radar systems are presented. The concepts of the radome and frequency selective surface are also reviewed. The main contents include important parameters of the antenna, and theory and design consideration of the array antenna. Various wideband antennas are introduced and their performances are demonstrated, including: (1) for the phased array radar, the slotted waveguide array antenna has been widely used in airborne and marine radar systems; (2) for the ground penetrating radar, TEM horn antenna, broadband monopole antennas, and adaptive bow-tie antenna are presented; (3) for the noise radar, ridged horns and log-periodic Yagi antenna are introduced; (4) for the UWB systems, radiation characteristics of two newly developed UWB antennas (a coupled sectorial loop antenna and a spiral antenna with Dyson-style balun) are demonstrated. Furthermore, the radome and frequency selective surface used to protect the antenna/radar systems are brought in, whose functions, requirements, structures, and performance evaluation are presented, including state-of-the-art designs. The design considerations and future trend of the radar antennas and associated devices have been discussed and suggeted. More detailed can be referred to given references.

The development of the wideband antenna technology triggers the advancement of the antenna in the radar system. The progress of the antenna design also reveals applications of many innovative materials and structures. Designing low-profile, ultra-wideband, and electrically small antennas have become one of the primary goals in the antenna society. Future radar systems will require ultra-wide/multi-band antennas with capabilities of high-speed, high resolution, and high reliability. Wideband antennas covering ELF-VLF and HF-UHF will be challenging but eagerly desired. Smart impedance matching network should integrate with the miniaturized wideband antennas to form high efficiency antenna system. Also, fast and low-cost conductive printing technology can assist antennas conformal to various mobile platforms and hence become invisible. These innovative technologies will benefit future radar systems that may initiate a new research field for the wideband antennas.

6. References

Allen, B. *et al. (2007). Ultra-wideband Antennas and Propagation for Communications, Radar and Imaging*, John Wiley & Sons, ISBN 0470032553, England.

Balanis, C. (1982). *Antenna Theory: Analysis and Design,* John Wiley & Sons, ISBN 047160352X, Hoboken, NJ.

Behdad, D. & Sarabandi, K. (2005). A compact antenna for ultrawide-band applications. *IEEE Trans. Antennas and Propagation,* Vol. 53, No. 7, July 2005, pp. 2185-2192.

Behdad, D. *et al*. (2009). A low-profile third-order bandpass frequency selective surface. *IEEE Trans. Antennas and Propagation,* Vol. 57, No. 2, February 2009, pp. 460-466.

Chen, T. (1957). Calculation of the parameters of ridge waveguides. *IRE Trans. Microwave Theory and Techniques,* Vol. 5, No. 1, January 1957, pp. 12-17.

Chung, B. & Lee, T. (2008). UWB antenna assists ground-penetrating radar. *Microwave & RF Magazine,* December 2008, pp. 59-65.

Hopfer, S. (1955). The design of ridged waveguides. *IRE Trans. Microwave Theory and Techniques,* Vol. 3, No. 5, October 1955, pp. 20-29.

Huff, G. & Roach, T. (2007). Stripline-based spiral antennas with integrated feed structures, impedance transformer, and Dyson-style balun, *IEEE Antennas and Propagation Society International Symposium*, pp. 2698-2701, Honolulu, HI, USA, June 2007.

Kozakoff, D. (1997). *Analysis of Radome-Enclosed Antennas*, Artech House, ISBN 0890067163, Norwood, MA.

Lai, C. & Narayanan, R. (2005). Through-wall imaging and characterization of human activity using ultrawideband (UWB) random noise radar, *Proc. SPIE Conference on Sensors, and Command, Control, Communications, and Intelligence (C3I) Technologies for Homeland Security and Homeland Defense IV*, vol. 5778, pp. 186–195, Orlando, FL, USA, March-April 2005.

Lestari, A. *et al*. (2005). Adaptive wire bow-tie antenna for GPR applications. *IEEE Trans. Antennas and Propagation,* Vol. 53, No. 5, May 2009, pp. 1745-1754.

Rudge, A. *et al*. (1983). *The Handbook of Antenna Design,* Vol. 2, IET, ISBN 0906048877, UK.

Mailloux, R. (2005). *Phased Array Antenna Handbook*, Artech House, ISBN 1580536905, Norwood, MA.

Milligan, T. (2004). A design study for the basic TEM horn antenna. *IEEE Antennas and Propagation Magazine*, Vol. 46, No. 1, February 2004, pp. 86-92.

Milligan, T. (2005). *Modern Antenna Design,* John Wiley & Sons, ISBN 0471457760, New York, NY.

Munk, A. (2000). *Frequency Selective Surface : Theory and Design,* John Wiley & Sons, ISBN 0471370479, New York, NY.

Sekretarov, S. & Vavriv, D. (2008), Circular slotted antenna array with inclined beam for airborne radar application, *Proceedings of the German Microwave Conference,* pp. 475-478, Hamburg, Germany, March 2008.

Skolnik, M. (1990). *Radar Handbook,* McGraw-Hill, ISBN 007057913X, New York, NY.

Skolnik, M. (2001). *Introduction to Radar Systems,* McGraw-Hill, ISBN 0072909803, New York, NY.

Stevenson, R. (1948). Theory of slots in rectangular waveguides. *J. App. Physics,* Vol. 19, 1948, pp. 24-38.

Volakis, J. *et al*. (2007). *Antennas Engineering Handbook,* McGraw-Hill, ISBN 0071475745, New York, NY.

Watson, W. (1949). *The Physical Principles of Waveguides Transmission and Antenna Systems*. pp. 122-154, Clarendon Press, Oxford.

Wisniewski, J. (2006). Requirements for antenna systems in noise radars, *International Radar Symposium 2006*, pp.1-4, Krakow, Poland, May 2006.

Wiesbeck, W. *et al.* (2009). Basic properties and design principles of UWB antennas. *IEEE Proceedings*, Vol. 97, No. 2, February 2009, pp. 372-385.

Wu, T. (1995). *Frequency Selective Surface and Grid Array,* John Wiley & Sons, ISBN 0471311898, New York, NY.

Radar Technology

Edited by Guy Kouemou

ISBN 978-953-307-029-2
Hard cover, 410 pages
Publisher InTech
Published online 01, January, 2010
Published in print edition January, 2010

In this book “Radar Technology”, the chapters are divided into four main topic areas: Topic area 1: “Radar Systems” consists of chapters which treat whole radar systems, environment and target functional chain. Topic area 2: “Radar Applications” shows various applications of radar systems, including meteorological radars, ground penetrating radars and glaciology. Topic area 3: “Radar Functional Chain and Signal Processing” describes several aspects of the radar signal processing. From parameter extraction, target detection over tracking and classification technologies. Topic area 4: “Radar Subsystems and Components” consists of design technology of radar subsystem components like antenna design or waveform design.

InTech Europe
University Campus STeP Ri
Slavka Krautzeka 83/A
51000 Rijeka, Croatia
Phone: +385 (51) 770 447
Fax: +385 (51) 686 166
www.intechopen.com

InTech China
Unit 405, Office Block, Hotel Equatorial Shanghai
No.65, Yan An Road (West), Shanghai, 200040, China
中国上海市延安西路65号上海国际贵都大饭店办公楼405单元
Phone: +86-21-62489820
Fax: +86-21-62489821

IntechOpen